Award Number: W81XWH-06-2-0067

TITLE: Alliance for Nanohealth Competive Research Program

PRINCIPAL INVESTIGATOR: Dr. Jodie L. Conyers

CONTRACTING ORGANIZATION: University of Texas Health Science Center
Houston, TX 77030

REPORT DATE: October 2011

TYPE OF REPORT: Final Addendum

PREPARED FOR: U.S. Army Medical Research and Materiel Command
Fort Detrick, Maryland 21702-5012

REPORT DOCUMENTATION PAGE

Form Approved
OMB No. 0704-0188

1. REPORT DATE *(DD-MM-YYYY)*	2. REPORT TYPE	3. DATES COVERED *(From - To)*
01-10-2011	Final Addendum	29 SEP 2009 - 28 SEP 2011

4. TITLE AND SUBTITLE
Alliance for Nanohealth Competive Research Program

5a. CONTRACT NUMBER

5b. GRANT NUMBER
W81XWH-06-2-0067

5c. PROGRAM ELEMENT NUMBER

6. AUTHOR(S)
Dr. Jodie L. Conyers

E-Mail: jodie.l.conyers@uth.tmc.edu

5d. PROJECT NUMBER

5e. TASK NUMBER

5f. WORK UNIT NUMBER

7. PERFORMING ORGANIZATION NAME(S) AND ADDRESS(ES)
University of Texas Health Science Center
Houston, TX 77030

8. PERFORMING ORGANIZATION REPORT NUMBER

9. SPONSORING / MONITORING AGENCY NAME(S) AND ADDRESS(ES)
U.S. Army Medical Research and Materiel Command
Fort Detrick, Maryland 21702-5012

10. SPONSOR/MONITOR'S ACRONYM(S)

11. SPONSOR/MONITOR'S REPORT NUMBER(S)

12. DISTRIBUTION / AVAILABILITY STATEMENT
Approved for Public Release; Distribution Unlimited

13. SUPPLEMENTARY NOTES

14. ABSTRACT

The Alliance for NanoHealth Competitive Research Program funded through this contract has supported up to 12 new collaborative research projects bridging the gaps between medicine and nanotechnology. In this final year of the program, emphasis was placed on characterization of nanoparticle assemblies for drug delivery and molecular imaging and using atomic force microscopy to characterize the interactions of such particles with living cells.

15. SUBJECT TERMS
No subject terms provided.

16. SECURITY CLASSIFICATION OF:			17. LIMITATION OF ABSTRACT	18. NUMBER OF PAGES	19a. NAME OF RESPONSIBLE PERSON
a. REPORT	b. ABSTRACT	c. THIS PAGE			USAMRMC
U	U	U	UU	19	19b. TELEPHONE NUMBER *(include area code)*

TABLE OF CONTENTS

Imaging nanoparticles using Atomic Force Microscopy

During the last year several imaging projects have been developed to visualize the effects and mechanics of nanovectors on the cell membrane structure. We have used a BioScope II^{TM} Controller (Bruker Corporation, Santa Barbara, CA) integrated with a Nikon TE2000-E inverted optical fluorescence microscope (Nikon Instruments, Inc. Lewisville, TX) located at the South Campus Research Building 3 at the University of Texas Health Science Center at Houston. A summary of the techniques employed and general results of our research are described next.

Project 1

Using Biological Atomic Force Microscopy to Image Gold-Labeled Liposomes at Human Coronary Artery Endothelial Cell Membranes.

Although atomic force microscopy (AFM) has been used extensively to characterize cell membrane structure and cellular processes such as endocytosis and exocytosis, the corrugated surface of the cell membrane hinders the visualization of extracellular entities, such as liposomes, that may interact with the cell. To overcome this barrier, we used 90 nm nano-gold particles to label FITC liposomes and monitor their endocytosis on human coronary artery endothelial cells (HCAECs). We were able to study the internalization mechanism, binding sites, and distribution of the gold-coupled liposomes, a novel delivery system, on endothelial cells by using AFM. We found that the gold-liposomes attached to the HCAEC cell membrane during the first 15-30 min of incubation, liposome cell internalization occurred from 30-60 min, and most of the gold-labeled liposomes had invaginated after 2 hr of incubation. Liposomal intake took place most commonly at the periphery of the nuclear zone. Pretreatment with Dynasore monohydrate, an inhibitor of endocytosis, obstructed the internalization of the gold-liposomes. This study showed the versatility of the AFM technique, combined with fluorescent microscopy, for investigating liposome uptake by endothelial cells and elucidating their binding mechanism. The 90 nm colloidal gold nano-particles proved to be a noninvasive contrast agent that efficiently improves AFM imaging during the investigation of biological nano-processes.

Liposome imaging

The liposomes were deposited on mica for AFM analysis by using a modification of the procedure of Ramachandran *et al*., [**1**]. Ruby red mica circles (11 mm diameter) were first glued to a 3" x 1" glass slide with Scotch super glue gel. Both uncopled liposomes and gold-coupled liposomes were left to stand on freshly cleaved mica during 10 min. The liposomes were then fixed with 10% neutral buffered formalin for 10 min, washed 3 times with ultrapure water (Barnstead water system, Thermo Scientific; Dubuque, IA), and dried in a sterilGARD III hood flow before scanning. AFM liposome imaging was performed in tapping mode in air with RTESP cantilevers (fo=262-325 kHz, k=20-80N/m).

Cell imaging

For the endocytosis studies, HCAECs were seeded in a collagen (50 µg/ml)-coated 8-well slide system to 80% confluence, with EBM-2 supplemented with an EGM-2 bullet kit (SingleQuots) and incubated 24 hrs at 37°C in a 5% CO_2 atmosphere. The cells were then treated with the gold-labeled liposomes at a final concentration of 1.525 mM (solution ratio 1:10 in culture medium) for four different incubation times (15, 30, 60, and 120 min) at 37°C. During the incubations, the slide chambers were agitated at 30 rpm with an Orbit P4 Digital Shaker (Labnet, Edison, NJ). The cells were then washed 3 times with culture medium to remove unbounded liposomes and fixed for 15 min with 10% neutral buffered formalin.

AFM studies were performed on 'never-dried' fixed cells, after the four incubation periods, to investigate liposome-membrane interactions. Liquid scanning was performed in contact mode with DNP-S cantilevers (f*o*=12-24 kHz, *k*=0.06 N/m). AFM was performed with a BioScope II™ Controller (Bruker Corporation). Image analysis was conducted with the Research NanoScope software version 7.30. For routine liposome detection, we used a Nikon TE2000-E inverted optical fluorescence microscope (Nikon Instruments, Inc. Lewisville, TX) integrated to the bioscope system. The cells that emitted a positive fluorescent signal by the FITC-labeled liposomes were selected for AFM scanning. The results from the liposome AFM measurements were also verified by DLS analysis.

Inhibition of endocytosis

The effect of Dynasore monohydrate on cellular uptake of liposomes was also investigated. Dynosore monohydrate is a GTPase inhibitor that targets dynamin and blocks endocytosis. The Dynasore monohydrate was initially diluted to 20 mM in DMSO (99.9%) and stored in 20-µl aliquots to -20°C. At the time of the experiments, it was diluted to 80 µM (0.4% DMSO) in EBM-2 that contained no serum or albumin [**2**]. The HCAECs were then treated with Dynasore monohydrate (80 µM) for 15 min and agitated at 30 rmp at 37ºC before being incubated for 60 min with gold-labeled liposomes diluted 1:10 (1.525 mM) in EBM-2 supplemented with the EGM-2 BulletKit. We chose to investigate Dynosore monohydrate's blocking effect after 60 min of incubation because, as described later, we learned that the 'gold-liposomes' had been taken up by the cells at that point in time. This is also in agreement with the work of Mastrobattista *et al*., [**3**], who reported that the 60% of cell-bound immunoliposomes are taken up by bronchial epithelial cells within 1 h of incubation.

RESULTS

Characterization of uncoupled liposomes and gold-coupled liposomes

The average diameter of the non-gold coupled liposomes, as determined by DLS, was 129 nm (**Figure 1A**), and a polydispersity index (PDI) of 0.126. For the gold-coupled liposomes (**Figure 1B**), the DLS results showed a major peak at 285 nm. The PDI for the gold-liposomes was 0.689. The polydispersity index indicates the variation in particle size. Its denomination can vary from 0 to 1. A value of 1 means that the sample is very polydisperse and a value of 0 that the particle size does not vary. Values below 0.2 indicate that a sample is monodisperse [**4**, **5**]. Therefore, the PDI values reported here indicate that the non-coupled liposomes were very monodisperse. However, the gold-coupled liposomes had a more heterogeneous formulation, some containing only one or two gold particles and some having many (clusters). The DLS results are the averages of three different measurements (13 runs each).

AFM analysis of liposomes

The structural properties of uncoupled and gold-coupled liposomes were analyzed using AFM. Both types of liposomes were imaged after fixation with 10% formalin to ensure the preservation of their original structure. AFM was performed in tapping mode in air with RTESP cantilevers. **Figure 2** shows a typical AFM image of non-gold coupled liposomes deposited on fresh cleaved mica and fixed with formalin. AFM analysis of these liposomes showed an average diameter of 121.5± 27 nm. This result was comparable to the diameter measurement obtained by DLS (129 nm).

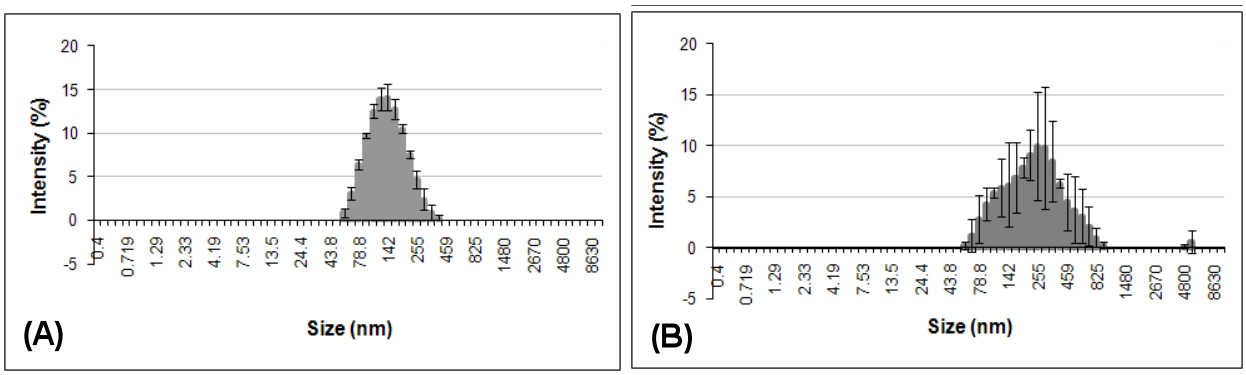

Figure 1. The hydrodynamic radii of non-coupled (A) and gold-coupled liposomes (B), estimated by DLS. Uncoupled liposomes (A) observed a mean diameter value of 129 nm. The size distribution for gold labeled liposomes (B) described a major peak for particles about 285 nm in size.

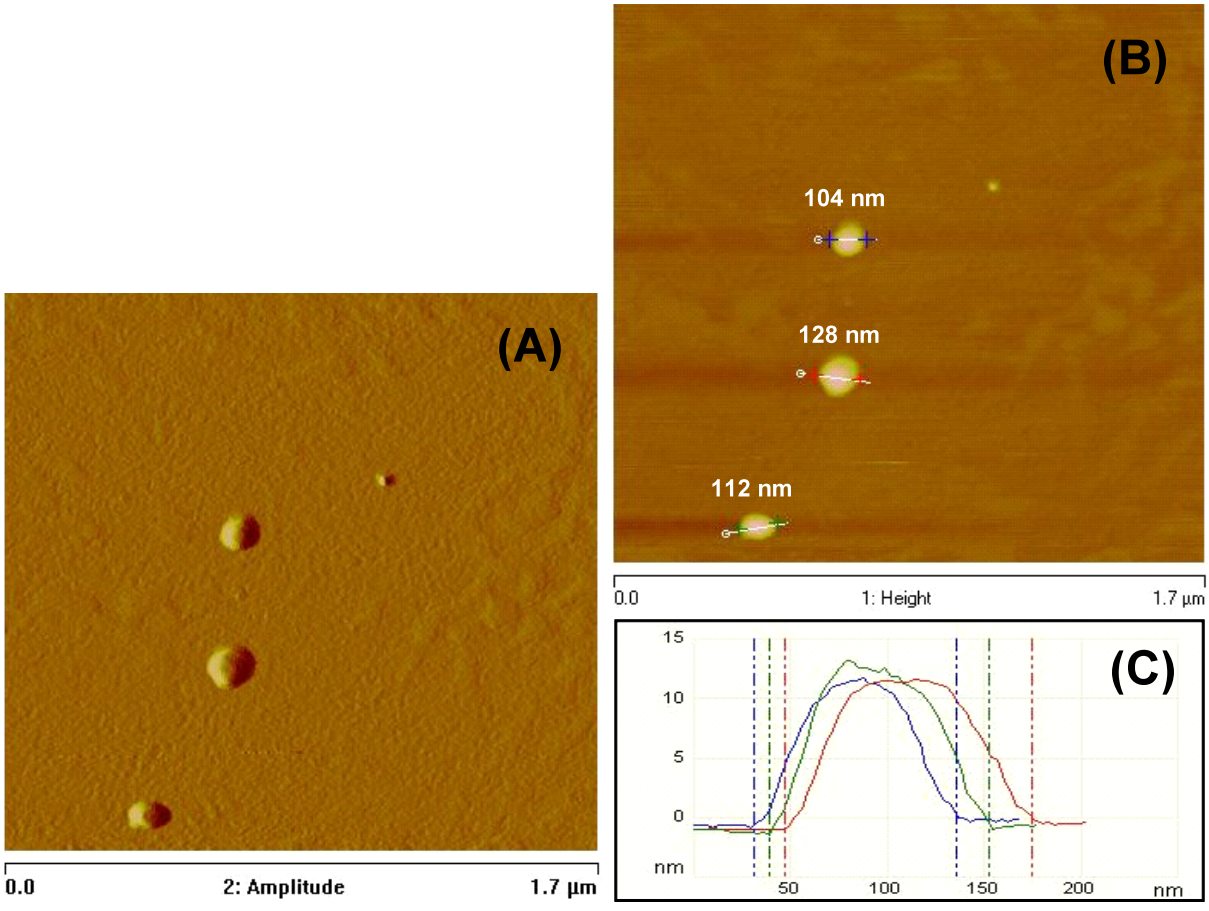

Figure 2. AFM images of non-gold coupled liposomes visualized in amplitude (A) and height (B) modes to 1.7 µm (x-y). The AFM section analysis (C) of these liposomes showed an average diameter of 121.5 ± 27 nm when deposited on mica and scanned in air. This result was comparable to that of the DLS analysis (129 nm). Scan obtained in tapping mode using RTESP tips (f*o*=262-325 kHz, *k*=20-80 N/m).

To enhance AFM imaging, nano-gold particles were covalently linked to FITC liposomes. **Figure 3** shows AFM imaging of the geometric structure of a typical gold-liposome cluster (303 nm diameter) composed of three particles with individual diameters of 95, 86, and 78 nm. According to DLS measurements, these gold-liposome complexes had an average size of 285 nm.

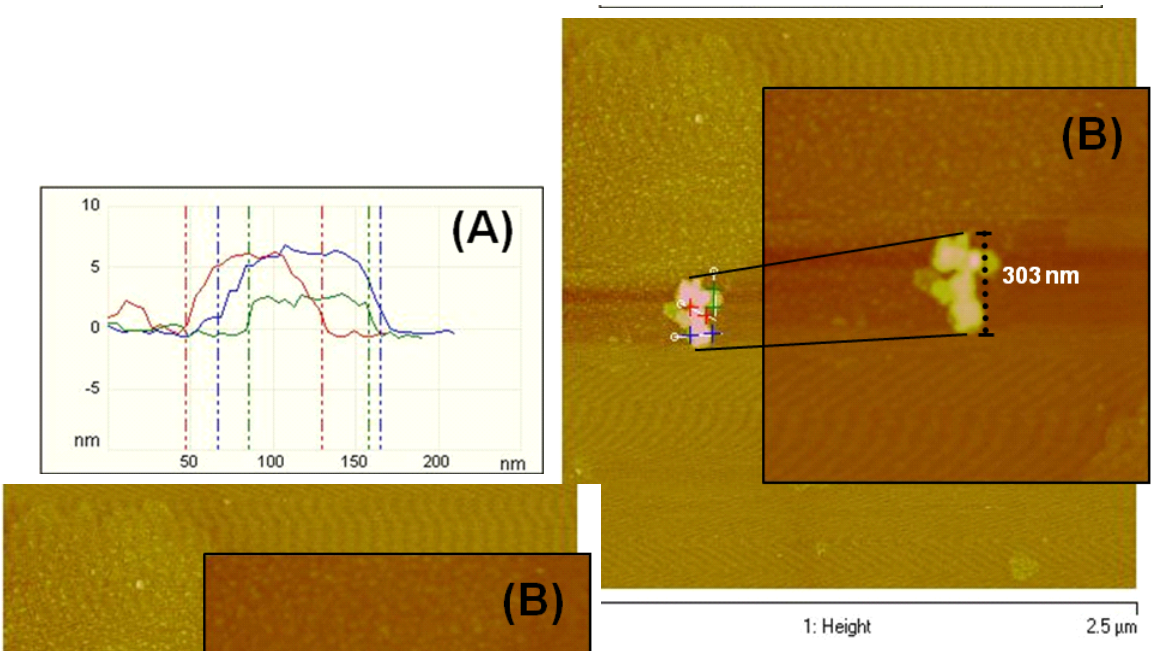

Figure 3. AFM images of FITC-labeled liposomes coupled to 90 nm gold particles and scanned on fresh cleaved mica. (A) AFM sectional analysis measuring the diameter of the particles (95, 86, and 78 nm) that made up a gold-liposome cluster. (B) Additional digital zoom to 1 µm² taken from the original scan at 2.5 µm (x-y). The DLS analysis showed that the gold-liposome complexes had a diameter of 285 nm. Tapping mode in air using RTESP cantilevers (f*o*=262-325 kHz, *k*=20-80 N/m).

Endocytosis and liposome coupling

The surface topology and characteristics of biological membranes can routinely be described using biological AFM instruments [**6**, **7**]. Nevertheless, the application of this technique has rarely been approached to resolve kinetics for liposome cell uptake. To investigate how endocytosis takes place within endothelial cells, we used 90 nm gold particles to track FITC-labeled liposomes. **Figure 4** shows sequential AFM images indicating how the 'gold-liposomes' penetrated the plasma membrane.

After 15 min of incubation (**Figure 4A** and **B**), some of the coupled liposomes were already attached to the cells. They still quivered when probed with the AFM tip during scanning (seen as liposome drifting in **Figure 4A**). Nevertheless, the 'gold-liposomes' were strongly bonded to the cell membrane at this

time, given that the liposomes remained attached to the cell when probed. At 30 min, the liposome clusters started to enter the cells (not shown). Actual endocytosis was seen in samples incubated for 60 min (**Figure 4C-D**). **Figure 4C** and **D** clearly show how the plasma membrane is enclosing the extracellular material and gradually engulfing it (see also **Figure 5A**, at a smaller scan area). The corresponding fluorescence images in **Figures 4D** and **5B** show strong positive signals of the two 'gold-liposome' clusters (indicated by arrows) that were selected for AFM scanning. One of these clusters was about 3.2 μm and the other 3.8 μm in diameter when they were half way through the cell membrane. Liposomes incubated with HCAECs for 120 min were almost completely internalized (**Figure 4E**). These studies demonstrated that using colloidal gold nano-particles as an image-enhancement tool did not hinder endocytosis and that uptake of the liposomes took place in 120 min. The time course of the endocytosis can be summarized as follows: liposome attachment to the plasma membrane (15-30 min), internalization (30-60 min), and membrane fusion (120 min). These results agree with the findings reported by Ramachandran *et al.,* [**1**], who studied endocytosis of cisplatin-encapsulated liposomes. In that study, the cisplatin produced liposomes significantly stiffer than non-encapsulated liposomes, which facilitated their detection by AFM scanning.

On the other hand, our negative controls (HCAEC incubated with 'gold-liposomes' for 60 and 120 min, which did not show signals detectable by fluorescence imaging) had smooth and even membrane surfaces (**Figure 5C** and **D**). Signs of elevated or raised areas were not present during AFM scanning, and the lack of fluorescence signaling indicated the absence of FITC-labeled gold-liposomes.

Blocking gold-liposome uptake

It was of particular interest to investigate if the internalization of the gold-coupled liposomes could be hindered by a typical inhibitor of endocytosis. We used Dynosore, a cell permeable, non-competitive dynamin 1 and dynamin 2 GTPase activity inhibitor, to block dynamin-dependent endocytosis of the liposomes. Our experiments indicated that the 'gold-liposome' clusters barely attached to the external walls of cells treated 15 min with 80 μM Dynosore and then incubated with the 'gold-liposomes' for 60 min. In most of the cases, the 'gold-liposomes' were easily removed from the cell membrane when probed with the AFM cantilever. The force loading exercised by the AFM probe scanning to a velocity of 30 μm/s, removed ~90% of the liposomes. This indicates poor binding with the plasma membrane and obstruction of the 'gold-liposome' uptake after Dynosore pre-treatments.

CONCLUSIONS

Ninety-nanometer colloidal gold particles are a useful noninvasive labeling agent for visualization by AFM of liposome uptake by HCAECs. We were able to visualize the movement of the gold coupled liposomes through the cell membrane before absorption. The time course of endocytosis was as follows: liposome attachment to the plasma membrane at 15-30 min, internalization at 30-60 min, and membrane fusion at 120 min. 'Gold-liposome' clusters up to ~3 μm in diameter can be efficiently taken up by endocytosis regardless of their geometric structure. The gold-coupled liposomes behaved as expected when exposed to an endocytosis inhibitor (Dynosore) to block their internalization process. The gold nanoparticles did not hinder liposome uptake. We successfully established a potential method to track biomolecules in complex systems using 90 nm colloidal gold nano-particles as a noninvasive contrast agent to improve AFM imaging.

We are currently conducting studies using similar approaches to compare immuno-liposomes bearing anti-intercellular adhesion molecule-1 with nonspecific immuno-liposomes. Both types of liposomes are coupled to nano-gold particles to determine their binding efficiency and mechanistic regulation of their internalization process. Experiments will be conducted on endothelial cells that have been induced into an inflammatory response. The purpose of using this technique is to investigate how specific immuno-liposomes interact with inflamed endothelium for an effective modulation of therapeutics on clinical trials.

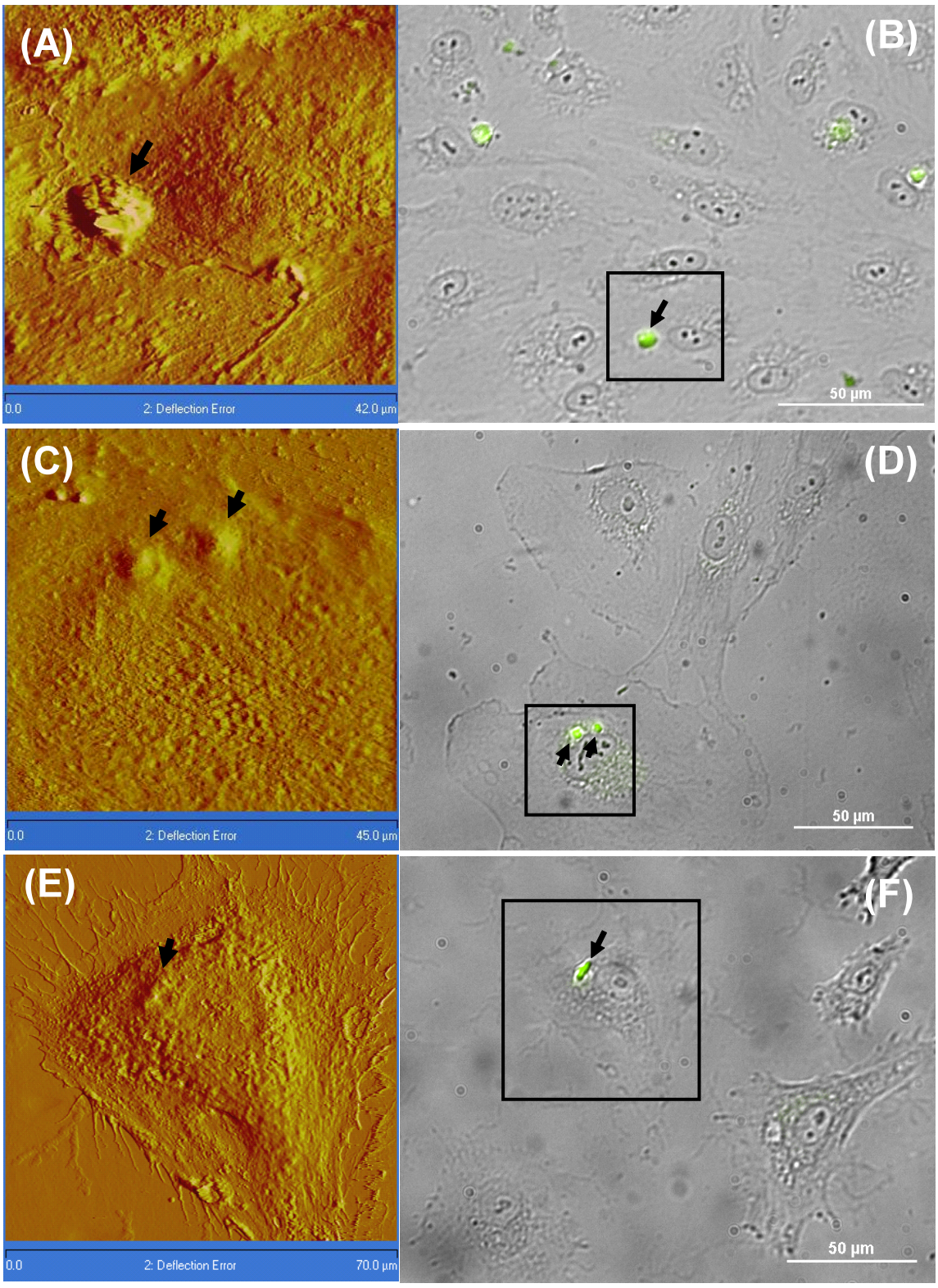

Figure 4.- AFM images (A, C, and E) and corresponding fluorescence images (B, D, and F) of HCAECs incubated for 15 (A and B), 60 (C and D), and 120 min (E and F) with FITC-labeled liposomes conjugated with 90 nm gold particles. The cells with positive signaling in the bright field images (squares in the right-hand panels) were selected for AFM scanning. (A) Typical AFM image of an HCAEC incubated for 15 min, showing a gold liposome cluster attached to the cell membrane. (C) AFM image demonstrating the internalization process occurring in an HCAEC incubated for 60 min with 'gold liposomes'. (E) The AFM micrograph of an HCAEC incubated for 120 min corroborated that the 'gold liposomes' internalized almost

completely at this time point. Cells fixed in formalin 10% and scanned in contact mode in liquid (DNP-S f*o*=12-24 kHz, *k*=0.06 N/m).

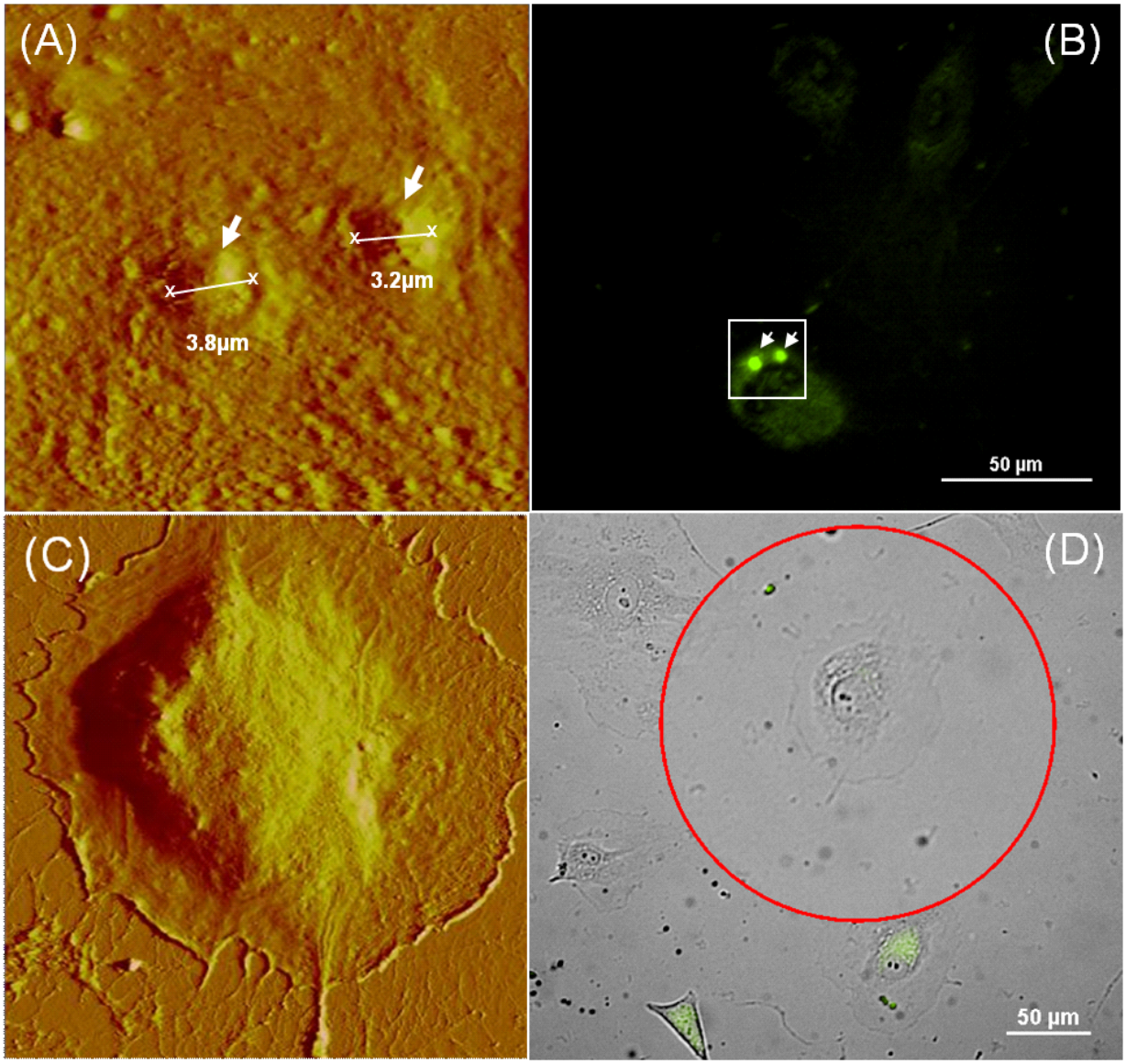

Figure 5. Liposome endocytosis occurring at 60 min of incubation (smaller scan area from Figure 4C). (A) AFM micrograph obtained at 25 µm (x-y) illustrating the engulfment of the 'gold liposomes' during cell membrane internalization. (B) The corresponding fluorescence image clearly shows the positive signaling emitted by the gold liposome clusters that were scanned. (C) AFM micrograph at 65 µm (x-y) of an HCAEC negative control showing a smooth and even membrane surface after 60 min of incubation with FITC-labeled gold-liposomes. (D) The cells with no signalling, which indicated the absence of 'gold-liposomes', were selected for scanning from the corresponding fluorescence images. Cells fixed in formalin 10% and scanned in contact mode in liquid (DNP-S f*o*=12-24 kHz, *k*=0.06 N/m).

REFERENCES

1. Ramachandran, S.; Quist, A. P.; Kumar, S.; Lal, R. *Langmuir.* **2006**, 22, 8156–8162.

2. Newton, A. J.; Kirchhausen, T.; Murthy, V. N. *PNAS.* **2006**, 103 (47), 17955–17960.

3. Mastrobattista, E.; Storm, G.; Bloois, L.; Reszka, R.; Bloemen, P. G.; Crommelin, D. J.; Henricks, P. A. *Biochim Biophys Acta.* **1999**, 1419 (2), 353–363.

4. Hengst, V.; Oussoren, C.; Kissel, T.; Storm, G. *Int J Pharm.* **2007**, 331 (2), 224–227.

5. Jackson, S. A.; Thomas, R. M., Eds. *Cross-sectional imaging made easy*. Churchill Livingstone: New York, **2004**. p. 3–16.

6. Puu, G.; Artursson, E.; Gustafson, I.; Lundström, M.; Jass, J. *Biosensors & Bioelectronics.* **2000**, 15, 31–41.

7. Ruspantini, I.; Diociaiuti, M.; Ippoliti, R.; Lendaro, E.; Gaudiano, M. C.; Cianfriglia, M.; Chistolini, P.; Arancia, G.; Molinari, A. *The Histochemical Journal,* **2001**, 33, 305–309.

Note: These results have actually been submitted to the *Langmuir* editorial office for publication.

05-Aug-2011

Manuscript successfully submitted to Langmuir.

Title: "Using Biological Atomic Force Microscopy to Image Gold-Labeled Liposomes at Human Coronary Artery Endothelial Cell Membranes"

Authors: Zaske, Ana; Danila, Delia; Golunski, Eva; Queen, Michael; Conyers, Jodie

Manuscript ID: la-2011-03059h.

Project 2

Probing the mechanical properties of TNF-α stimulated endothelial cell with atomic force microscopy.

TNF-α (tumor necrosis factor-α) is a potent pro-inflammatory cytokine that regulates the permeability of blood and lymphatic vessels. The plasma concentration of TNF-α is elevated (> 1 pg/mL) in several pathologies, including rheumatoid arthritis, atherosclerosis, cancer, pre-eclampsia; in obese individuals; and in trauma patients. To test whether circulating TNF-α could induce similar alterations in different districts along the vascular system, three endothelial cell lines, namely HUVEC, HPMEC, and HCAEC, were characterized in terms of 1) mechanical properties, employing atomic force microscopy; 2) cytoskeletal organization, through fluorescence microscopy; and 3) membrane overexpression of adhesion molecules, employing ELISA and immunostaining. Upon stimulation with TNF-α (10 ng/mL for 20 h), for all three endothelial cells, the mechanical stiffness increased by about 50% with a mean apparent elastic modulus of E ~5 ± 0.5 kPa (~3.3 ± 0.35 kPa for the control cells); the density of F-actin filaments increased in the apical and median planes; and the ICAM-1 receptors were overexpressed compared with controls. Collectively, these results demonstrate that sufficiently high levels of circulating TNF-α have similar effects on different endothelial districts, and provide additional information for unraveling the possible correlations between circulating pro-inflammatory cytokines and systemic vascular dysfunction.

Cell culture and TNF-α treatment

In order to investigate the influence of TNF-α on the cell membrane elasticity, HCAEC, HUVEC, and HPMEC were seeded in a 60 mm culture dish to 80% confluence, with EBM-2 medium supplemented with an EGM-2 BulletKit and incubated for 24 h at 37°C in a 5% CO_2 atmosphere. The cells were then treated with 3 mL of TNF-α (10 ng/mL) for 20 h to promote an inflammatory response [**1**]. Culture dishes were later rinsed with EBM-2 media to wash out the TNF-α solution. Data were taken at room temperature in a liquid atmosphere.

Cells (4×10^4 cells/well) were grown in EBM media supplemented with an EGM-2 Bullet Kit (Cambrex) at 37 °C in 5% CO_2. ICAM-1 was expressed on the surface of the HCAEC, HUVEC and HPMEC by activating the cells with 10 ng/ml TNF-α for 20 hours, and the extent of ICAM-1 expression was assessed by ELISA. For ELISA, the cells were incubated with TNF-α (10 ng/ml) for 20 hours at 37 °C and 5% CO_2 in a 96-well plate. The next day, the cells were washed with PBS, fixed with Formalin for 20 minutes at room temperature, incubated with 3% BSA and 0.1% Tween 20 for 1 hour and then incubated with anti-ICAM antibody (1:1,000 dilution in PBS, v/v) for 2 hours at 25 °C. The unbound anti-ICAM antibody was removed from the activated HCAEC by washing with PBS and the cells were incubated with anti-mouse IgG 2b (γ-2b)-peroxidase (1:2,000 dilution in PBS, v/v) for 1 hour at room temperature. The excess of secondary antibody was washed away with PBS and then ABTS substrate (100 μl) was added. After 30 minutes of incubation, the absorbance at 405 nm was measured with a Tecan plate reader. Non-activated cells were also subjected to ELISA as controls.

Atomic force microscopy

A Bioscope II Atomic force microscope (Bruker, Santa Barbara, CA) combined with a fluorescence microscope (TE-2000; Nikon, Melville, NY) was used for testing and imaging the cells. The AFM probe consisted of a 5 µm diameter silica particle (colloidal probe) attached at the edge of silicon nitride V-shaped cantilevers (Novascan, Ames, IA) (**Figure 1**). Data were acquired with NanoScope software (version 7.30; Bruker). A schematic representation of the cantilever tip interacting with a cell membrane and the geometrical features of the colloidal probe are shown in **Figure 1**. The relatively large particle size led to larger contact areas and more evenly distributed contact pressures, which limit the penetration depth upon contact and provide average information [**2**]. The cantilever spring constant was calibrated using thermal tuning and resulted in values from 0.1 to 0.3 N/m with less than ~8% of error [**3**] in EBM-2 cell culture media (nominal value of 0.32 N/m).

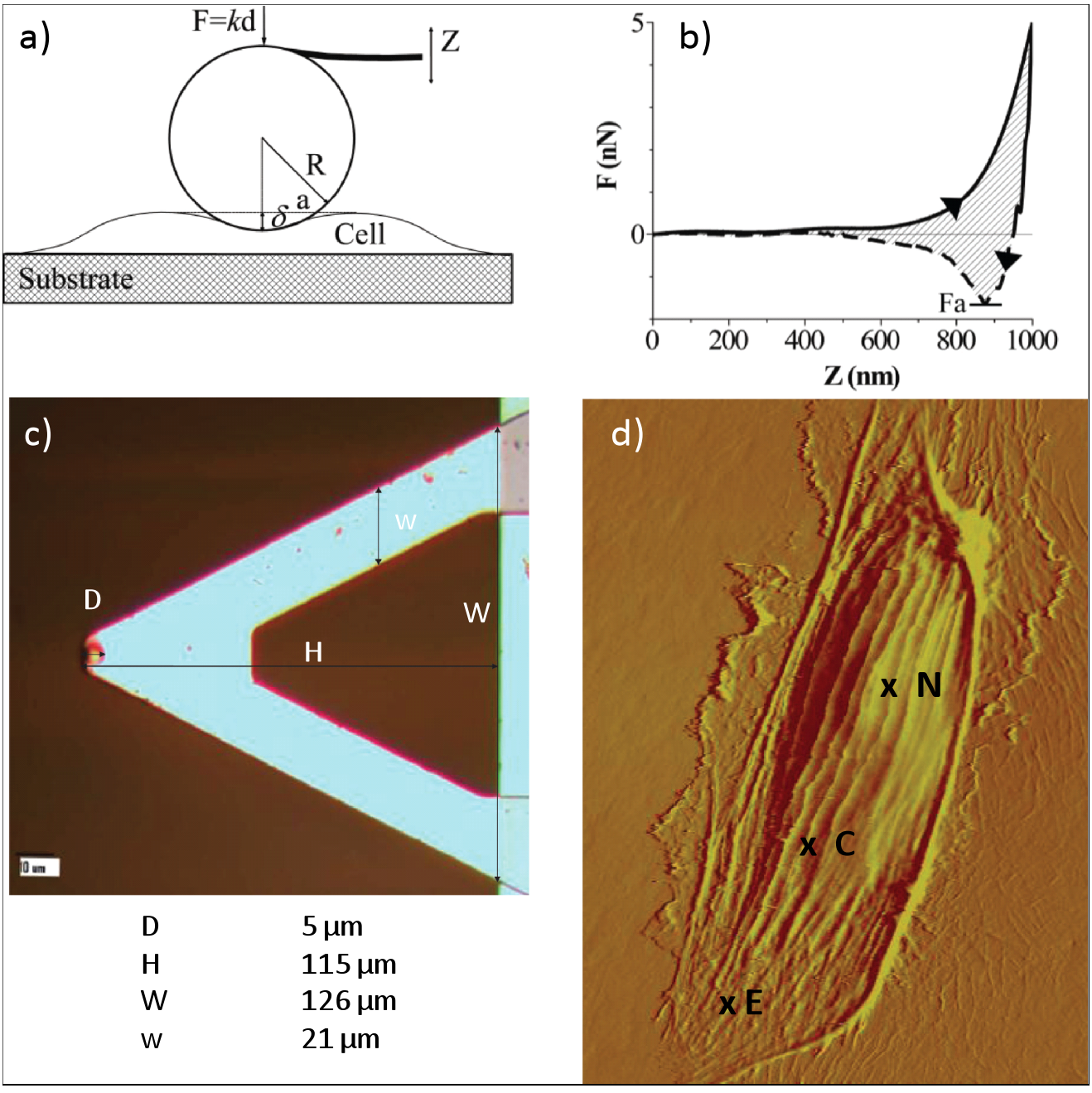

Figure 1. Atomic force microscopy for the mechanical characterization of live cells. a) Schematic of the colloidal probe (spherical particle attached at the tip of a cantilever beam) interacting with the cell membrane adhering over a rigid substrate. b) A representative force-displacement curve with a measurable force of adhesion Fa and area ratio Av. c) Microscopy image and geometrical data for the V-shaped cantilever beam with a colloidal probe of D = 5 μm in diameter; d) AFM micrograph of a HCAEC scanned alive to 120 μm (X-Y) in EBM-2 media at room temperature. Contact mode in liquid (DNP-S f*o* = 12–24 kHz, k = 0.06 N/m). Abbreviations: N, nucleus; C, contact area; E, edge.

RESULTS

Effects of TNF-α stimulation on the apparent elastic modulus The apparent compressive elastic moduli were calculated by analyzing the force-displacement curves obtained through AFM following the Hertzian contact theory. The same procedures were applied to all three ECs in both the unstimulated (control) and stimulated conditions. A typical force-displacement curve is shown in **Figure 1b**, where the dashed line corresponds to the approaching curve and the solid line to the retracting curve. The curves were measured over relatively flat regions of the cell membrane (point C in **Figure 1d**), always sufficiently far from the cell nucleus (point N in **Figure 1c**) and edge (point E in **Figure 1c**). The force-displacement curves were recorded in the same location of the cell, and the apparent elastic modulus were very consistent, exhibiting small standard deviations over multiple measurements. All the force-displacement curves were obtained for an indentation force F_{ind} of 0.5 nN and an approaching/retracting probe velocity v_{ind} of 0.25 μm/sec. For such small values of Find and v_{ind}, the assumptions of the Hertzian theory are fully satisfied [**4**]: the indentation depth was always smaller than 200 nm (sufficiently smaller than the thickness of the cell) and the viscoelastic response of the cell membrane was negligible. The presence of a cell under the probe was monitored in situ through an optical microscope.

The apparent elastic moduli for the three cell lines are presented in the bar chart of **Figure 2**, and related table, for both un-stimulated (white bars) and stimulated (dark bars) conditions. It was measured E = 3.44 ± 0.64 kPa for the HUVECs, E = 3.07 ± 0.36 kPa for the HCAECs and E = 3.42 ± 0.77 kPa for the HPMECs in the un-stimulated condition. There was no statistically significant difference between the apparent elastic modulus of the three cell lines ($P < 0.05$), giving an average E = 3.31 ± 0.35 kPa. This result is in good agreement with other analysis available in the literature, conducted on endothelial cells following the same procedures [**4**]. Also, these results confirm that cells performing similar functions (endothelial cells) but located in different organs do exhibit the same apparent elastic modulus and, consequently, similar cytoskeletal organization.

About 20 hours after stimulation with TNF-α, force-displacement curves were recorded and analyzed to derive the apparent elastic moduli E = 5.39 ± 0.63 kPa for the HUVECs, 4.72 ± 1.15 kPa for the HCAECs and 4.84 ± 0.89 kPa for the HPMECs. Compared to the un-stimulated cells a statistically significant increase ($P < 0.01$) in the apparent modulus is observed for all cell lines with a ratio (Es/Eu) between stimulated (Es) and un-stimulated (Eu) cells of 1.54, 1.42 and 1.56 respectively for HCAECs, HPMECs and HUVECs. In other words, an increase in cell stiffness of about 50% is observed upon stimulation with 10 ng/ml of TNF-α over 20 hours leading to an average E = 4.98 ± 0.53 kPa.

The measurement of the apparent elastic modulus is influenced by the force applied over the cell membrane and by the velocity of the probe. A sensitivity analysis was performed on E by varying the indentation force Find between 0.5 and 2 nN and the indentation velocity v_{ind} between 0.25 and 0.1 μm/sec. The results of such analysis confirmed the importance of reducing F_{ind} and v_{ind} for accurately

estimating the compressive modulus. Different methods have been proposed to extract the mechanical properties of cells, such as magnetic [**5**] and optical [**6**] tweezers, micropipettes [**7**] in addition to atomic force microscopy. Generally, the methods and the procedures affect the final measure giving different mechanical properties for the same cell type. Nonetheless, it is here important to emphasize that the present work aims at a comparative analysis rather than to an absolute measurement of the cellular mechanical properties.

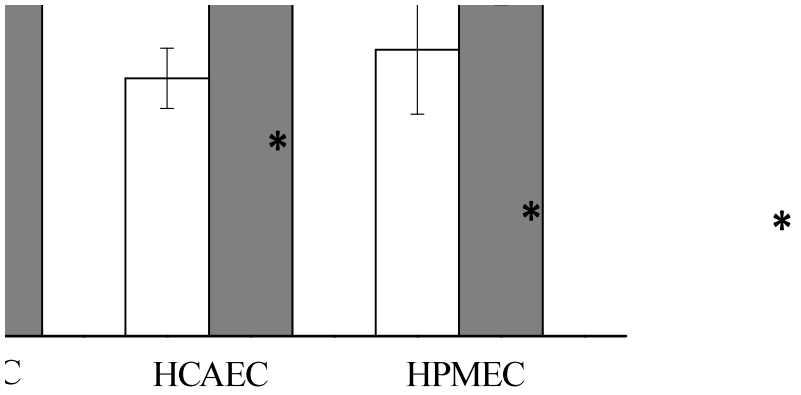

Figure 2. Apparent elastic modulus for three different endothelial cell lines. Bar chart presenting the apparent elastic modulus *E* for HUVEC, HCAEC, and HPMEC under unstimulated (control) and stimulated (20 h with 10 ng/mL TNF-α) conditions. (*Find* = 0.5 nN; *vind* = 0.25 μm/s; **P* < 0.05; number of cells *n* = 3; repetitions per cell *N* > 30).

Effects of TNF-α stimulation on the force of adhesion and viscoelastic response

In addition to the apparent elastic modulus, the adhesive force at the interface between the colloidal probe and the cell membrane and the viscoelastic response of the cell were recorded. The force of adhesion F*a* was estimated as the maximum force measured along the retracting curve (**Figure 1b**), following standard procedures [**8**]; whereas the viscoelastic response was quantified as the ratio (A*v*) between the energy dissipated due to viscoelastic losses (area between the approaching and retracting curves – dashed area in **Figure 1b**) and the overall mechanical work performed (area under the approaching curve) [**8**].

Since, the AFM probe was not decorated with any ligand molecules, interfacial adhesion was only associated with weak non-specific interactions. This was reflected by the negligibly small values of F*a* (<< 1 nN) measured with low indentation forces Find (= 0.5 nN) and velocities v_{ind} (= 0.25 μm/s). In all the experiments, the retracting curves appeared as continuous with no noticeable abrupt jumps, generally

associated with the breakage of specific molecular bonds, thus confirming the non-specific nature of the forces at the probe-cell interface. Therefore, in order to generate appreciable adhesive forces and viscoelastic losses, the indentation force and the retracting velocity were increased up to F_{ind} = 5.0 nN and v_{ret} = 40.0 μm/s, respectively.

For the un-stimulated HUVECs and HCAECs an adhesion force (area ratio A*v*) of, respectively, 1.32±0.30 nN (1.50±0.14) and 1.26±0.31 nN (1.47±0.37) was measured with no statistically significant difference ($P < 0.01$); whereas significantly smaller was the adhesion force (area ratio) estimated for the un-stimulated HPMECs with a value of 0.24±0.10 nN (0.74±0.13). It is interesting to observe that under physiological conditions, the viscoelastic losses associated with the endothelial cells of the pulmonary microvasculature are about 50% smaller than those associated with the umbilical and coronary endothelial cells. Indeed, the lung microvasculature, following the respiratory cycle, is continuously subjected to compression and expansion, and a smaller area ratio A*v* would imply lower viscoelastic losses possibly reflecting a natural evolution of the system towards a more energetically efficient operation.

More interestingly, for the stimulated cells, no significant difference was observed among the three cell lines ($P < 0.01$) with a force of adhesion (area ratio A*v*) of, respectively, 0.55±0.22 nN (1.08±0.22) for the HUVECs, 0.54±0.17 nN (1.02±0.13) for the HCAECs and 0.46±0.09 nN (0.74±0.13) for the HPMECs. The force of adhesion and viscoaelastic losses for the HUVECs and HCAECs decreased significantly (50%) upon stimulation with TNF-α, whereas an opposite trend was observed for the HPMECs. In the Supporting Information, a sensitivity analysis is presented elucidating the effect of the retracting velocity on the force of adhesion and viscoelastic losses. It is confirmed that the viscoelastic response of the cell membrane decreases as the retracting velocity reduces.

CONCLUSIONS

The mechanical properties of three different cell lines (HUVEC, HCAEC and HPMEC) were analyzed before and after stimulation with the pre-inflammatory cytokine TNF-α. The analysis revealed that (i) before stimulation with TNF-α no significant difference exists in terms of apparent compressive modulus among the three vascular districts with a mean value E = 3.30 ± 0.35 kPa; (ii) upon stimulation with TNF-α, the stiffness of the endothelial cells increases by about 50%, a mean value reaching E = 5 ± 0.5 kPa; (iii) before stimulation with TNF-α, the viscoelastic losses in the pulmonary microvasculature are about 50% lower than in the other two districts considered, for which no significant statistical difference was observed; (iv) upon stimulation with TNF-α, the viscoelastic losses becomes statistically similar in all three vascular districts. To the author's knowledge, this is the first work that analyze the effect of TNF-α, on three different endothelial districts and the results presented could provide additional information for unraveling the possible correlations between pro-inflammatory cytokines (as TNF-α) and systemic vascular dysfunction.

REFERENCES

1. Danila D, Partha R, Elrod DB. Et al. Antibody-labeled liposomes for CT imaging of atherosclerotic plaques: in vitro investigation of an anti-ICAM antibody-labeled liposome containing iohexol for

molecular imaging of atherosclerotic plaques via computed tomography. *Tex Heart Inst J. 2009:*36(5):393-403
2. Iyer S, Gaikwad RM, Subba-Rao V, et al. Atomic force microscopy detects differences in the surface brush of normal and cancerous cells, *Nat. Nanotech*. 2009:4:389-393
3. HJ Butt, Jaschke M., Calculation of thermal noise in atomic force microscopy. *Nanotechnology* 1995:6:1-7
4. Mathur AB, Collinsworth AM, Reichert WM, et al. Endothelial, cardiac muscle and skeletal muscle exhibit different viscous and elastic properties as determined by atomic force microscopy. *J Biomech*. 2001:34(12):1545-53
5. Bausch AR, Möller W, Sackmann E. Measurement of local viscoelasticity and forces in living cells by magnetic tweezers. *Biophys J*. 1999:76:573-9
6. Wei MT, Zaorski A, Yalcin HC, et al. A comparative study of living cell micromechanical properties by oscillatory optical tweezers. *Opt Express*. 2008:16(12):8594-603
7. Sato M, Theret DP, Wheeler LT, et al. Application of the micropipette technique to the measurement of cultured porcine aortic endothelial cell viscoelastic properties. *J Biomech Eng. 1990:*112(3):263-8.
8. Attard P. Measurement and interpretation of elastic and viscoelastic properties with the atomic force microscope. *J. Phys.: Condens. Matter* 2007:19:473201

Note: This investigation has been published in the *International Journal of Nanomedicine* 6: 179–195.

January-2011

Title: "Probing the mechanical properties of TNF-α stimulated endothelial cell with atomic force microscopy"
Authors: LEE, SEI-YOUNG; **ANA-MARIA ZASKE**; TOMMASO NOVELLINO; DELIA DANILA; MAURO FERRARI; JODIE CONYERS; PAOLO DECUZZI.

Project 3

Nanotoxicity: characterizing early stage alterations in cell biomechanical response

Increasing use of nanomaterials has engendered *in vitro* toxicological studies which mostly rely on metabolic and biocompatibility assays. Complimentary testing procedures are needed to assess possible alterations in cell functions at the early stage of cell-nanomaterial interaction. Here, we test the dose-dependent biomechanical response of HPMECs exposed for 24h with commercially available gold nanoparticles (AuNPs), of 30 and 100 nm in diameter. Four non-conventional characterization studies were performed aiming at the analysis of the i) cytoskeletal organization; ii) adhesion and morphology of the cell; and iii) stiffness of the cell membrane. For both cells and both particle sizes, as the AuNP concentration increases, the actin network in the cell cytoskeleton undergoes a progressive reorganization observing thicker, denser and less spatially organized filaments. This is accompanied by a reduction in i) cell area coverage, up to 70%; ii) Young's modulus, up to 20% in the perinuclear region where most of the AuNPs accumulate; and iii) adhesion propensity under flow. Consistently, the rolling velocity of the cells is observed to increase significantly with the AuNP concentration. No appreciable decrease in cell viability was measured, at 24h. These results demonstrated that alterations in cell cytoskeleton occur at the early stage of cell-nanoparticle interaction, and induce dose-dependent dysfunctions in the biomechanical response of the cell.

(Manuscript is in preparation for publication).